

Electronic structure of some β -($C_{10}H_8S_8$) $_2X$ compounds as studied by infrared spectroscopy

C. S. Jacobsen and D. B. Tanner*

Physics Laboratory III, Technical University of Denmark, DK-2800 Lyngby, Denmark

Jack M. Williams, U. Geiser, and H. H. Wang

Chemistry Division and Materials Science Division, Argonne National Laboratory, Argonne, Illinois 60439-4843

(Received 17 December 1986)

Polarized reflectance measurements have been made on two isostructural conducting compounds of bis(ethylenedithio)tetrathiafulvalene [BEDT-TTF or ET, ($C_{10}H_8S_8$)]: β -(ET) $_2$ AuI $_2$ and β -(ET) $_2$ I $_2$ Br. The former is superconducting at ambient pressure with $T_c = 5$ K, whereas the latter retains normal-metal conductivity to low temperatures. The reflectance measurements, made at temperatures of approximately 30 and 300 K, spanned 80 cm^{-1} (0.01 eV) through $33\,000\text{ cm}^{-1}$ (~ 4 eV); they were made for polarization along the ET molecular stacking axis and transverse to it in the sheets or layers of ET molecules. Band-structure parameters determined from the plasmon frequencies imply that the anisotropy is rather low for organic conductors, with $t_{\parallel} \approx 0.22$ eV and $t_{\perp} \approx 0.09$ eV for β -(ET) $_2$ AuI $_2$; $t_{\parallel} \approx 0.18$ eV and $t_{\perp} \approx 0.07$ eV for β -(ET) $_2$ I $_2$ Br. At 300 K, the spectra differ substantially from the expectations of simple one-electron models, suggesting that both electron-phonon and electron-electron interactions play important roles in the electronic structure of these materials. At low temperatures, the materials display basically metallic characteristics, yet deviate significantly from simple Drude-model behavior. At 30 K, no effect attributable to superconducting fluctuations could be observed.

I. INTRODUCTION

In the study of superconductivity in organic solids, a particular group of materials based on the molecule bis(ethylenedithio)tetrathiafulvalene [$C_{10}S_8H_8$ (BEDT-TTF or in short, ET)] has attracted considerable interest in the last few years. The materials in focus are of the sort (ET) $_nX_m$, where X can be one of several inorganic monovalent anions and n and m are in the range 1–3. In 1982 (ET) $_2$ ClO $_4$ -(C $_2$ H $_3$ Cl $_3$) $_{0.5}$ (a compound which also contains trichloroethane solvent molecules) was reported¹ metallic to 1.4 K. Superconductivity was first detected² in a particular phase of (ET) $_2$ ReO $_4$, at pressures above 4.5 kbar and temperatures below 2 K. The first ambient pressure superconductor in the ET family was discovered in 1983, when (ET) $_2$ I $_3$ in its triclinic β phase was reported³ to have a transition temperature $T_c \sim 1.4$ K. Since then it has been found⁴ that T_c is extremely pressure sensitive, increasing to ~ 8 K at > 0.5 kbar. It has been shown^{5–7} that T_c remains high (8 K) if the pressure is released at low temperatures and the samples are not warmed above 125 K. Other ambient-pressure superconductors based on ET include^{8–10} γ -(ET) $_2$ (I $_3$) $_{2.5}$ ($T_c \cong 2.5$ K), β -(ET) $_2$ IBr $_2$ ($T_c \cong 2.8$ K), and β -(ET) $_2$ AuI $_2$ ($T_c \cong 5$ K). All these findings were rather surprising because in the β -(ET) $_2X$ family the room-temperature conductivity is rather low,³ about $30\ \Omega^{-1}\text{ cm}^{-1}$, corresponding to conduction-electron mean free paths much shorter than a lattice constant. Ordinarily, organic conductors with such low room-temperature conductivities become insulating at low temperatures.

As in other organic conductors, the ET molecules are organized in stacks, with considerable intrastack π -orbital overlap. The anions are closed shell and do not contribute

to the low-frequency conductivity. An additional feature of the ET compounds follows from the large number of sulfur atoms on the ET molecule and the many short ($d_{S-S} < 3.60$ Å, the van der Waals radius sum of S) interstack contacts.^{1,2,11,12} In the β -phase compounds the interstack contacts are short and the conductivity³ and thermoelectric power¹³ vary by no more than a factor of 2 in the a - b plane, the plane which contains the sheets of interacting ET chains. Other important features¹¹ of these 2:1 compounds are (1) an organization of the stack in interacting dimers, which may just be a consequence of the stoichiometry, and (2) a tilt of the normal to the ET molecules away from the stacking axis [$\sim 28^\circ$ in β -(ET) $_2$ AuI $_2$].

The electronic band structure may either be thought of as quarter-filled holelike referring to one ET molecule as a unit, but then with a considerable dimerization gap in the middle, or more correctly as a half-filled band based on the dimer as a unit and with a very close lying, filled lower band. Available band-structure calculations^{14,15} suggest a closed, cylindrical Fermi surface.

Previous infrared and optical studies on β -(ET) $_2X$ compounds have mostly centered on the room-temperature properties of the I $_3^-$ compound,^{16–20} but the discovery²¹ of qualitative changes with temperature has spurred further investigations.^{22,23} All studies report pronounced quasimetallic behavior in the stacking direction at 300 K (a well-defined plasma edge), but overdamped behavior perpendicular to the stacks (slow rise in reflectance towards low frequencies). At low temperatures plasma edges are found in both polarizations,^{22–24} but the spectra do not follow simple Drude behavior.

The aim of the present paper is to present optical spectra extending to far infrared frequencies, for two novel members of the isostructural β -(ET) $_2X$ family, namely¹⁰

β -(ET)₂AuI₂ and²⁵ β -(ET)₂I₂Br. The AuI₂⁻, or diiodoaurate, anion is a linear, symmetric, pseudohalide, (IAuI)⁻; β -(ET)₂AuI₂ has $T_c \approx 5$ K at ambient pressure. In contrast, β -(ET)₂I₂Br has a nonsuperconducting (measured to 0.45 K by rf penetration²⁵), metallic ground state. The absence of superconductivity in the latter material is believed to be due to disorder in the orientation of the asymmetric I₂Br⁻ ions,²⁵ i.e., (IIBr)⁻ or (BrII)⁻. We shall further compare the results with earlier data²¹ on β -(ET)₂I₃ ($T_c \approx 1.4$ K, ambient pressure). A preliminary presentation of our measurements has appeared.²⁴

II. EXPERIMENT

All measurements were done on individual single crystals of the distorted hexagon morphology, electrocrystallized from trichloroethane or tetrahydrofuran.¹² The samples had high-quality optical (001) faces of typical areas 1–2 mm².

These highly opaque samples are conveniently studied by means of near-normal-incidence, polarized reflectance measurements. The optical axes in the infrared range were determined as those directions yielding the maximum anisotropy when the polarizer was rotated. As previously found,^{16,21–23} these axes correspond to the stacking axis $a+b$ (\parallel), and a direction in the (a,b) plane perpendicular to the stacks (\perp). All subsequent measurements were carried out along these directions, although in the triclinic crystals in question the principal axes may well rotate at high frequencies, where intramolecular excitations in ET and/or ET⁺ and counterions²⁰ dominate the spectra. However, the intraband absorption which involves the charge carriers is at much lower frequencies than these high-frequency absorptions.

Data were accumulated in the 60–35 000-cm⁻¹ frequency range using three different instruments. The far infrared 60–700 cm⁻¹, was covered with a Bruker IFS113V Fourier-transform spectrometer equipped with an A510 reflectance attachment, a wire grid polarizer on polyethylene, and He-cooled Ge bolometer. A Perkin-Elmer model 98 grating monochromator was used in the 400–5000 cm⁻¹ mid infrared range with conventional mirror optics, a grid polarizer on AgBr, and a Golay cell detector. Finally, the high-frequency range was covered with a low-resolution Perkin-Elmer 98 fused quartz prism monochromator with Glan-Thompson prism polarizers, and PbS cell/photomultiplier as detectors. Gold and aluminum mirrors were used as reference in the infrared and visible, respectively.

Low-temperature spectra were obtained by thermally anchoring the sample to a temperature-controlled cold finger. Radiation shields with suitable holes reduced the amount of 300-K radiation reaching the samples, but in the present measurements the lowest attainable sample temperatures were²⁶ ~ 30 K.

III. RESULTS

A. Reflectance data

In Fig. 1 we show the broadband room-temperature reflectance of β -(ET)₂I₂Br. For \parallel as well as \perp polarizations

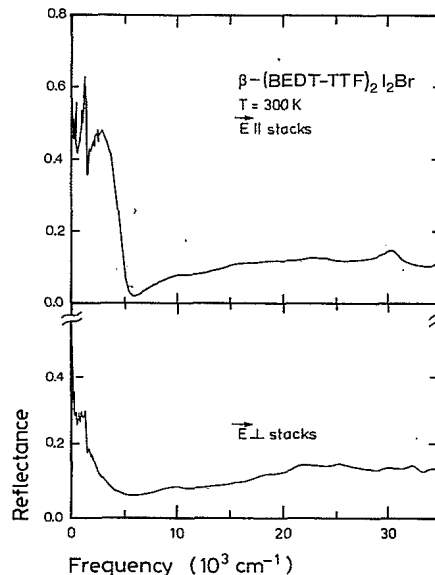


FIG. 1. Polarized reflectance of β -(ET)₂I₂Br from the far infrared to the near ultraviolet ($T=300$ K).

the reflectance is fairly low ($< 15\%$) above ~ 6000 cm⁻¹ with a number of weak dispersions at 10×10^3 , 16×10^3 , 23×10^3 , and 30×10^3 cm⁻¹ for \parallel and 10×10^3 , 18×10^3 , 22×10^3 , 25×10^3 , and 32×10^3 cm⁻¹ for \perp . Approaching low frequencies, a well-developed plasma edge is present in the \parallel polarization, but it is noted that the vibronic structure below 2000 cm⁻¹ is very pronounced. For the \perp polarization the rise is more gradual, corresponding to overdamped plasmon behavior where the relaxation rate is comparable to or exceeds the plasmon frequency. The overall features are typical for all the compounds.

In the following we describe the infrared part of the reflectance spectra as a function of material and temperature. Figures 2(a) and 2(b) present the stacking axis reflectance to 8000 cm⁻¹ for β -(ET)₂AuI₂ and $-I_2Br$ at $T=300$ and 30 K. Common features include the plasma edge around 5000 cm⁻¹, which sharpens and is slightly blue-shifted on cooling, and pronounced non-Drude structure in the range of molecular vibrations (< 2000 cm⁻¹). Differences between the two materials are (1) a higher position of the plasma edge in the AuI₂⁻ material, and (2) in the same compound a higher reflectance level below 2000 cm⁻¹ at 30 K. Also, the detailed shape in the vibrational lines differs, although, for example, the rather strong, split bands at ~ 400 cm⁻¹ and ~ 1300 cm⁻¹ are present in both 300-K spectra.

In Figs. 3(a) and 3(b) we show the results for E \perp stacks. The overdamped response at 300 K changes at 30 K to a reasonably well-defined plasma minimum in both materials, at 4000 cm⁻¹ in the AuI₂⁻ and at 3500 cm⁻¹ in the I₂Br⁻ compounds, respectively. The former shows pronounced non-Drude behavior at 30 K below 1000 cm⁻¹, whereas the latter displays a gradual rise in reflectance with decreasing frequency, more in accordance with expectations for a metal. The chain-axis vibrational line near 400 cm⁻¹ is absent in all transverse spectra, whereas

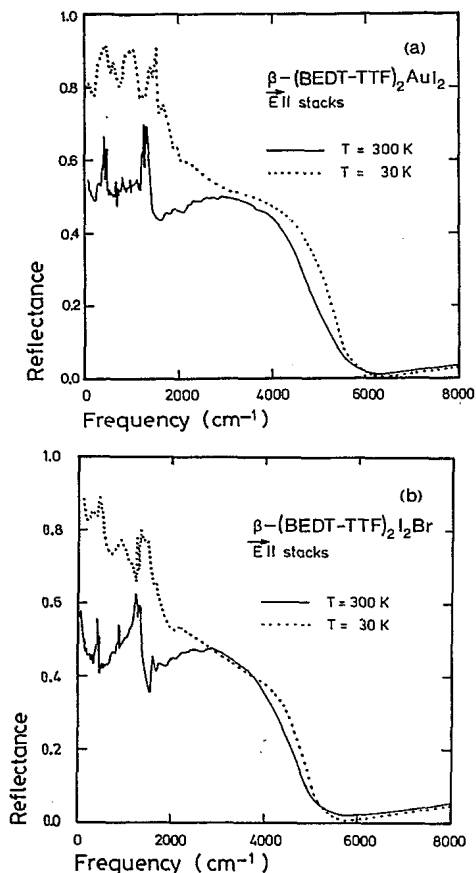


FIG. 2. Infrared stacking axis reflectance of (a) β -(ET)₂AuI₂ and (b) β -(ET)₂I₂Br, shown at two temperatures, $T=30$ and 300 K, respectively.

the 1300 cm⁻¹ structure is present in the 300-K I₂Br⁻ data although weaker than along the stacks.

Figures 4 and 5 show details of the far-infrared reflectance as a function of temperature. In both polarizations it is evident that the AuI₂⁻ data show distinct deviations from simple Drude behavior in the frequency range below 400 cm⁻¹. For $\vec{E} \parallel$ stacks it is noteworthy how the strong doublet at 430–460 cm⁻¹ is barely visible at low temperatures. This apparent change need not signal a change in oscillator strength, but may well be due to the change in background dielectric function (see below). For $\vec{E} \perp$ stacks the complete absence of the doublet is again noted. Apart from the non-Drude features discussed already, it is also clear that the 400–500 cm⁻¹ level rises faster with decreasing temperature in the AuI₂⁻ compound than in the I₂Br⁻ compound.

B. Kramers-Kronig analysis: σ and ϵ

The polarized reflectance spectra presented above have been analyzed by means of Kramers-Kronig transformation with the phase shift on reflection calculated according to²⁷

$$\theta(\omega) = \frac{\omega}{\pi} P \int_0^{\infty} \frac{\ln R(\omega')}{\omega^2 - (\omega')^2} d\omega' \quad (1)$$

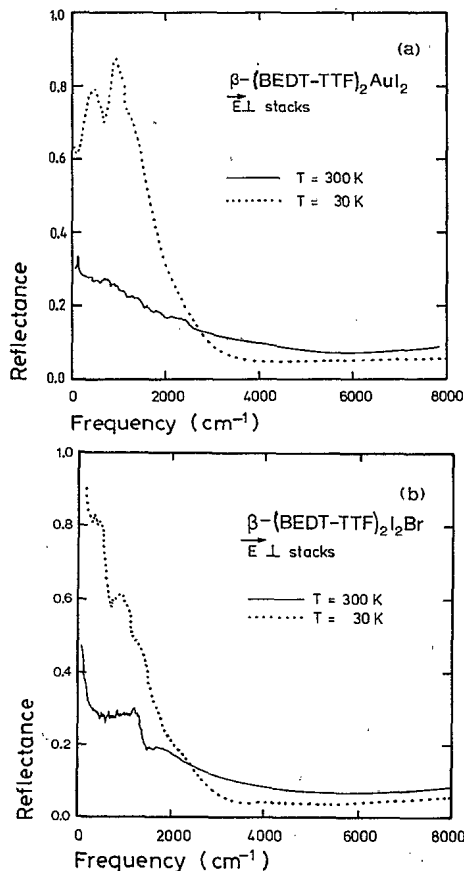


FIG. 3. Infrared reflectance for $\vec{E} \perp$ stacks of (a) β -(ET)₂AuI₂ and (b) β -(ET)₂I₂Br, shown at two temperatures, $T=30$ and 300 K, respectively.

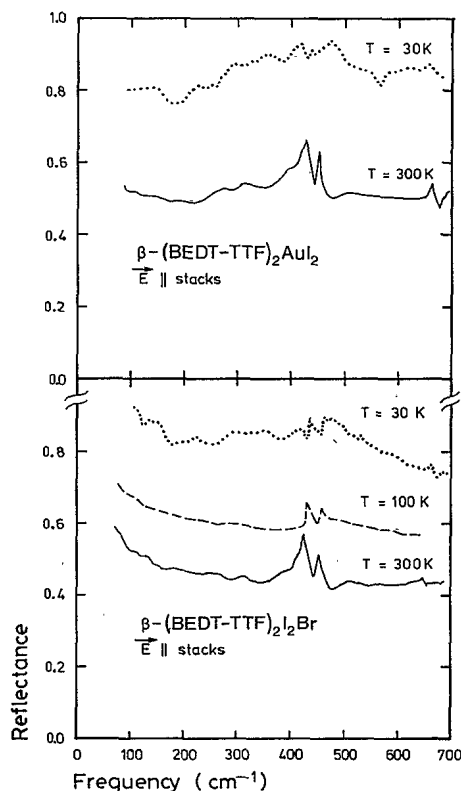


FIG. 4. Far-infrared stacking axis reflectance of β -(ET)₂AuI₂ and β -(ET)₂I₂Br, for temperatures from 30 to 300 K.

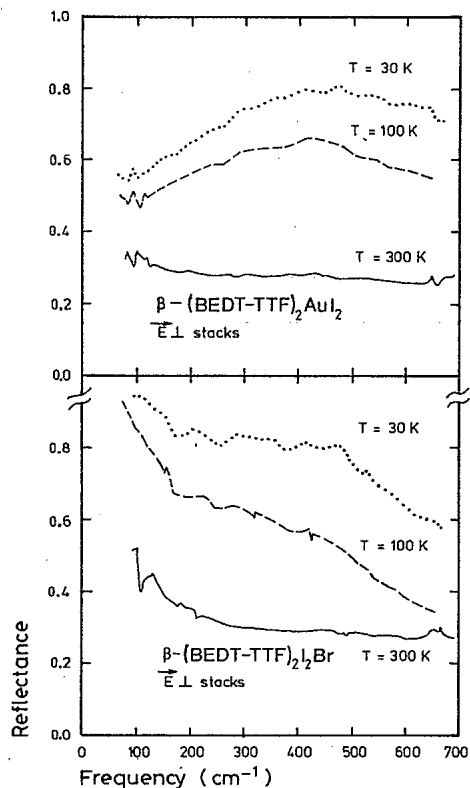


FIG. 5. Far-infrared reflectance for E|| stacks of β -(ET) $_2$ AuI $_2$ and β -(ET) $_2$ I $_2$ Br, for temperatures from 30 to 300 K.

The response functions $\epsilon(\omega)$ and $\sigma(\omega)$ are then given by

$$\epsilon(\omega) + i \frac{\sigma(\omega)}{\omega \epsilon_0} = \frac{1 + \sqrt{R(\omega)} e^{i\theta(\omega)}}{1 - \sqrt{R(\omega)} e^{i\theta(\omega)}} \quad (2)$$

In Eq. (1) it is in principle necessary to know $R(\omega)$ at all frequencies. The present study covers a frequency range of approximately 2.5 orders of magnitude around the range of primary interest. With Hagen-Rubens [Drude-like: $R(\omega) = 1 - A\omega^{1/2}$] extrapolations at low frequency, and representative extrapolations at high frequencies [$R(\omega) \propto (\omega_0/\omega)^d$, $d=0-1$, to 10^5 cm^{-1} and $d=4$ beyond], the results in the infrared are expected to be rather reliable.²⁷ The position of absorption bands should also be well-reproduced beyond the infrared, but the intensity distribution (oscillator strength) in that region may be influenced by the details of the extrapolation scheme adopted.

As an example of the broad frequency behavior we present again the 300-K results for β -(ET) $_2$ I $_2$ Br, now as conductivity from 80–34 000 cm^{-1} , Fig. 6. The band below 8000 cm^{-1} in both polarizations is the basic absorption related to the dc conductivity. This band is discussed in more detail below. The absorption features from 16 000 cm^{-1} and up may with a fair degree of certainty be assigned to internal, excitonlike transitions in either²⁰ ET $^+$ or I $_2$ Br $^-$. The lowest molecular ET $^+$ excitations are expected to be polarized in the plane of the molecule. We note that the long axis of the molecule has no

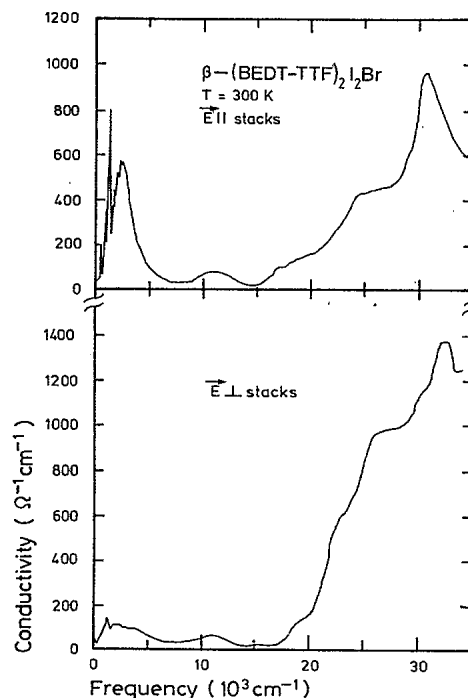


FIG. 6. Frequency-dependent conductivity of β -(ET) $_2$ I $_2$ Br from the far infrared to the near ultraviolet. Data are shown for $T=300$ K and for E|| stacks and E \perp stacks.

component along the \perp polarization. Thus the bands observed in that polarization (at $\sim 19 \times 10^3$, 23×10^3 , 26×10^3 and 33×10^3 cm^{-1}) are presumably due to absorption in I $_2$ Br $^-$ or to higher lying transitions in ET $^+$ with polarization perpendicular to the long axis. The bands polarized parallel to the chains (at $\sim 16 \times 10^3$, 24×10^3 , and 31×10^3 cm^{-1}) may similarly be assigned to long-axis transitions or to I $_2$ Br $^-$ excitations.

The origin of the 11 000- cm^{-1} band observed in both polarizations is less clear. One suggestion is that such low-lying bands in general²⁸ can be interpreted as originating from charge-transfer processes creating doubly occupied states (thus basically measuring the on-site Coulomb interaction U). However, for the low charge density in question, the intensity of this band should be vanishing,²⁹ and it is indeed not observed in systems such as²⁶ (TMTSF) $_2$ X and (TMTTF) $_2$ X, which have similar carrier densities. The main structural difference is that the organic molecules are nearly perpendicular to the stacks in the latter materials in contrast to the situation here. This difference hints that the 11 000- cm^{-1} band arises from mixing between the charge-transfer process and low-lying intramolecular excitations. Such an explanation has previously been proposed for similar absorptions in TCNQ compounds.³⁰

In the following we shall concentrate on the infrared part of the spectrum. The frequency dependent conductivity is shown in Figs. 7(a) and 7(b) and 8(a) and 8(b) for the two materials, two temperatures, and two polarizations. In both materials the stacking axis spectrum has about three times as much oscillator strength as the trans-

verse one. Another common feature is evident in all these results: At room temperature $\sigma(\omega)$ shows a broad peak around 2200 cm^{-1} with vibrational structure on the low-frequency side. At low temperature the oscillator strength moves down in frequency so the spectra become more Drude-like. Although there is still sharp fine structure, $\sigma(\omega)$ peaks well below 500 cm^{-1} . The room-temperature spectra for the two materials are rather similar, except for the absence of significant fine structure in the 1500–2000 cm^{-1} range for β -(ET)₂AuI₂, E \perp stacks. At low temperature $\sigma(\omega)$ reaches higher conductivity levels in β -(ET)₂AuI₂, but this material also shows the most marked deviations from Drude behavior at very low frequencies (far infrared).

The characteristic change with temperature of the spec-

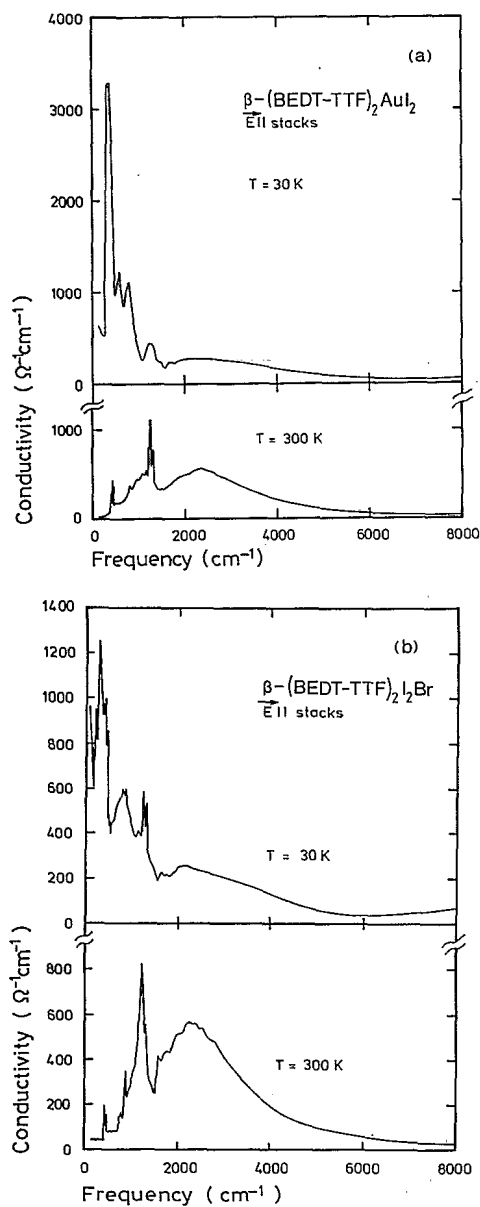


FIG. 7. Infrared stacking axis conductivity of (a) β -(ET)₂AuI₂ and (b) β -(ET)₂I₂Br, shown at two temperatures, $T=30$ and 300 K, respectively.

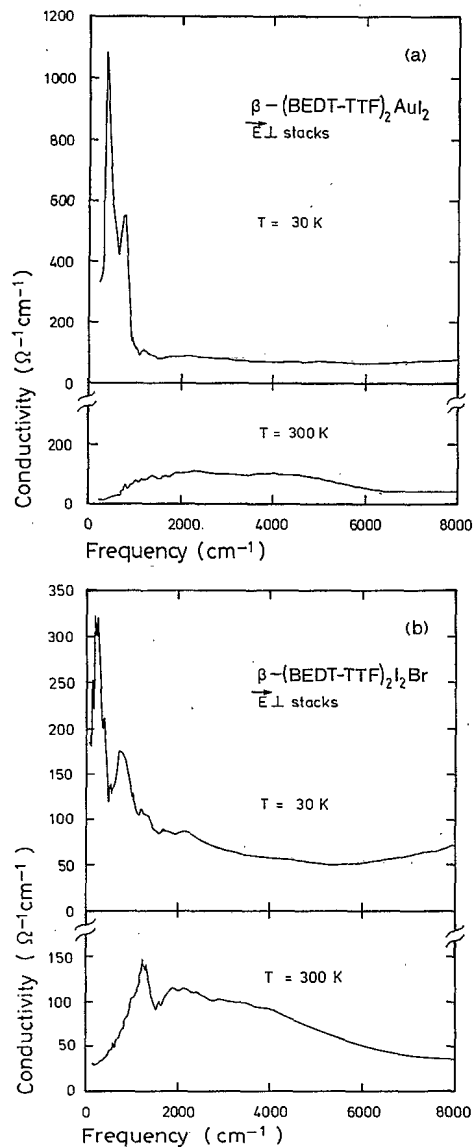


FIG. 8. Infrared conductivity for E \perp stacks of (a) β -(ET)₂AuI₂ and (b) β -(ET)₂I₂Br, shown at two temperatures, $T=30$ and 300 K, respectively.

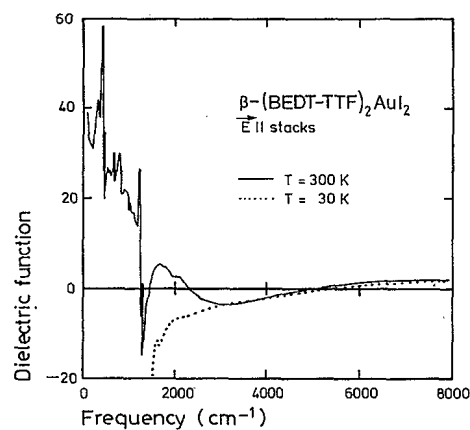


FIG. 9. Stacking axis dielectric function for β -(ET)₂AuI₂ in the infrared, at two temperatures, $T=30$ and 300 K, respectively.

tra, previously noted in²¹ β -(ET)₂I₃, is also reflected in $\epsilon(\omega)$, exemplified by the E_{||} stacks spectra in β -(ET)₂AuI₂ in Fig. 9. The 300-K spectrum is semiconductorlike with a number of zero crossings and positive values at low frequencies. In contrast, the 30-K spectrum only displays a single zero crossing (in the plasma edge region) and stays negative at lower frequencies. This negative $\epsilon(\omega)$ is the strongest evidence that at low temperatures these compounds have a basically metallic character. The zero crossing, identifying the plasmon frequency, only increases $\sim 5\%$ on cooling in spite of the rather drastic changes at low frequencies.

IV. DISCUSSION

A. Band structure and infrared properties

In contrast to most other highly conducting organic crystals, the molecular chains in β -(ET)₂X materials show a fair degree of dimerization. Thus, to think of them as quarter-filled band systems with a small dimerization gap at midband may not be appropriate.^{14,15} Indeed, in Ref. 17 the infrared properties of β -(ET)₂I₃ were analyzed in terms of a half-filled conduction band based on the ET dimer as the fundamental unit. Both intraband and interband (across the dimerization gap) contributions are found in this model, with the broad peak at 300 K in $\sigma(\omega)$ attributed to the interband portion. This peak occurs at an energy which can be explained in terms of a band-structure model, but the model also predicts the intraband (Drude-like) contribution to be considerably bigger than observed, when the data are extended to the far infrared (Ref. 21 and this work). Thus the broad structure at 300 K in the 2000–3000 cm⁻¹ range appears to possess a larger fraction of the oscillator strength than expected from one-electron theory. At low temperature we find (Figs. 7 and 8) that at least half of the oscillator strength in the broad band shifts to lower frequencies. The remaining part could very well be due to the interband transitions,²² but the shifting part must be given a different interpretation.

Here we will take the view that organic conductors such as the ET compounds are fairly strongly interacting systems with respect to the short-range electron-electron and electron-phonon interactions. Evidence for this interpretation comes from the quite low 300-K dc conductivity (mean free path for carriers much shorter than a lattice constant) and from the non-Drude frequency dependent conductivity, which resembles that of Peierls insulators,³¹ Hubbard-type Wigner crystals,³² or small polaron systems.³³ Organic conductors have a variety of external as well as internal (i.e., molecular vibration type of) phonons coupled to the electrons, which in combination with an appreciable short range Coulomb repulsion could lead to an efficient localization of the carriers on the dimers in the high-temperature regime. The true difficulty here is in understanding the transition to excellent metallic behavior with delocalized carriers at low temperature and the approximate T^2 dependence in the low frequency conductivity over the entire temperature range.³⁴

In analyzing the infrared spectra, we will first neglect the anomalous behavior and assume that the response near the plasmon frequency is insensitive to the non-Drude behavior so often observed at low frequencies [cf. the $\epsilon(\omega)$ temperature dependence discussed above]. This approach usually leads to reasonable band-structure parameters³⁵ within a rather crude band-structure model.

Thus, we neglect all details and simply introduce average transfer integrals, $t_{||}$ and t_{\perp} in an orthorhombic model:

$$E(k_{||}, k_{\perp}) = -2t_{||}\cos(k_{||}d_{||}) - 2t_{\perp}\cos(k_{\perp}d_{\perp}). \quad (3)$$

Here, $d_{||}$ is the mean molecular repeat distance along the stacks and d_{\perp} the stack repeat distance perpendicular to the stacks in the (a, b) plane. Obviously $t_{||}$ is an average value, and t_{\perp} is a weighted average of several interchain transfer integrals appearing in a more detailed triclinic band model. However, $t_{||}$ and t_{\perp} should still fairly represent the overall degree of anisotropy.

We proceed by fitting the Drude model for reflectance:

$$R(\omega) = \left| \frac{\sqrt{\bar{\epsilon}(\omega)} - 1}{\sqrt{\bar{\epsilon}(\omega)} + 1} \right|^2, \quad (4)$$

with

$$\bar{\epsilon}(\omega) = \epsilon_c - \frac{\omega_p^2}{\omega(\omega + i\gamma)}, \quad (5)$$

to the observed plasma edges at low temperature in order (1) to determine the zero crossings in $\epsilon(\omega)$, which are the plasmon frequencies $\Omega_p \simeq \omega_p / \sqrt{\epsilon_c}$ and (2) then to get the unscreened plasma frequencies ω_p by estimating the core dielectric constant ϵ_c . Standard RPA equations²¹ for the connection between ω_p , crystallographic data, and the transfer integral subsequently yield the values given in Table I, where data for β -(ET)₂I₃ have been included to allow comparison.

All three materials have $t_{||}:t_{\perp} \simeq 2.5:1$, a rather modest anisotropy for organic conductors. This anisotropy corresponds within the simple model of Eq. (3) to a closed, cylindrical Fermi surface, but is not far from the crossover to an open Fermi surface.

Among the materials, the AuI₂⁻ compound appears to have the largest transfer integrals as also evident from direct inspection of the plasma edges. With comparable anisotropies in β -(ET)₂AuI₂ and β -(ET)₂I₃ it follows that the Fermi level density-of-states $N(0)$ is bigger in the latter compound, which is consistent with a higher superconducting transition temperature,

$$T_c = (\hbar\omega_{ph}/k_B) \exp[-1/N(0)V],$$

assuming otherwise unchanged parameters ω_{ph} and V .

The actual value of $N(0)$ will depend rather sensitively on the details of the band structure. In our crude model, $N(0) \simeq 2.5 \text{ eV}^{-1}$ (per molecule, both spin orientations) for β -(ET)₂I₃ [2.1 eV^{-1} for β -(ET)₂AuI₂]. In comparison, data for the I₃⁻ compound of paramagnetic susceptibility³⁶ χ_s and low-temperature electronic specific heat³⁷ C_{el} would in a noninteracting electron-gas model lead to $N(0) = 5.6$ and 5.0 eV^{-1} , respectively. The rather big

TABLE I. Unscreened plasma frequencies and average transfer integrals for some β -(ET)₂X compounds at $T \approx 30$ K. Data for $X = \text{I}_3^-$ are from Ref. 21. $\epsilon_c = 3.6-4.0$.

X	$\omega_{p }$ cm ⁻¹	$d_{ }$ Å	$\omega_{p\perp}$ cm ⁻¹	d_{\perp} Å	$t_{ }$ eV	t_{\perp} eV
I ₃ ⁻	9600	4.62	5700	6.11	0.19	0.08
I ₂ Br ⁻	9300	4.59	5300	6.11	0.18	0.07
AuI ₂ ⁻	10300	4.55	5800	6.12	0.22	0.09

difference from the optical value suggests that χ_s is enhanced by Coulomb correlations (as frequently occur in organic conductors). C_{el} is presumably considerably enhanced by the electron-phonon interaction.³⁷

In systems with considerable electron-electron interactions, the intraband absorption is generally reduced as compared to what is expected from the noninteracting electron gas.³⁵ This decrease follows from a simple sum rule on the optical absorption,³⁸ and can be used as a measure for the interaction strength. In Table II we compare the estimated integrated oscillator strength,

$$I_{\sigma} = \frac{2}{\epsilon_0 \pi} \int_{\text{intraband}} \sigma(\omega) d\omega, \quad (6)$$

with ω_p^2 from Table I. In the absence of interactions, and provided the absorption is located well below ω_p , the two numbers should agree. Instead, we find in all cases a significant difference, which could be taken to indicate short-range interactions of the order of the bandwidth.³⁵ This result is consistent with χ_s being enhanced 2–3 times.

B. Spectral features in the infrared

We now discuss the distribution of oscillator strength in the infrared. Although the overall qualitative change with temperature is difficult to explain, some of the sharper features are readily understood as arising from the electron-molecular vibration coupling. For a nondegenerate orbital only the fully symmetric A_g modes couple to the conduction electrons.³⁹ The most important A_g modes are listed in Table III (Ref. 40). The A_g modes are not ordinarily infrared active. However, for a nonuniform molecular chain, they may by the symmetry lowering borrow intensity from the electrons resulting in spectral features with intensities related to the coupling strengths. The central C=C stretching modes at 1300 cm⁻¹ are

TABLE II. Integrated intraband oscillator strength for β -(ET)₂X, $T \approx 30$ K, as compared with ω_p^2 . Data on β -(ET)₂I₃ from Ref. 21.

X	I ₃ ⁻	I ₂ Br ⁻	AuI ₂ ⁻
$\omega_{p }^2$ (10 ⁷ cm ⁻²)	9.2	8.7	10.6
$I_{\sigma }$ (10 ⁷ cm ⁻²)	6.2	5.7	7.9
$\omega_{p\perp}^2$ (10 ⁷ cm ⁻²)	3.3	2.8	3.4
$I_{\sigma\perp}$ (10 ⁷ cm ⁻²)	2.0	1.8	2.2

known to couple strongly in TTF-like molecules.⁴¹ Indeed, strong vibrational effects in this range are visible in all the stacking axis spectra (Figs. 4 and 7); the broken symmetry presumably arises from the dimerization. In the perpendicular direction the molecules have equivalent positions, hence the vibrational features are expected to be weak, consistent with the observed spectra (Figs. 5 and 8), although the strongly coupled C=C modes are visible in the β -(ET)₂I₂Br spectra. A possible cause is the disorder introduced by the I₂Br⁻ ions.²⁵ [In β -(ET)₂AuI₂ the counterions are ordered.] Very similar observations may be made for the 430–460 cm⁻¹ doublet, although in this case it is hardly visible in the E₁ (stacks) spectra for any of the compounds.

The low-temperature, far infrared conductivity spectra of highly conducting organic metals constitute a somewhat controversial subject.⁴² Different experimental groups do not always agree on their findings, but in a majority of cases the results point to the existence of narrow modes of possible collective origin centered at zero frequency⁴² (i.e., the dc conductivity much exceeds what a reasonable extrapolation of the far infrared data would suggest.) In a few cases the low-frequency rise can be followed in a limited frequency range.⁴² In the present materials, although the far infrared is quite non-Drude, the extrapolated dc conductivities are in rather good agreement with measured values. Thus no narrow modes are implied at the temperatures investigated. The 35-GHz stacking axis conductivity has for example been measured³⁴ for β -(ET)₂AuI₂: $\sigma_{||}(T) \propto T^2$ and $\sigma_{||}(30 \text{ K}) \approx 300 \Omega^{-1} \text{ cm}^{-1}$ [compare Fig. 7(a)].

Thus the non-Drude low-temperature behavior is attributed to strong interaction effects, both electron-electron and electron-phonon (-vibration). That the stronger non-Drude character in the low-temperature β -(ET)₂AuI₂ spectra is a superconducting phenomenon seems rather unlikely, since it would imply strong fluctuations to 30 K in a material with $T_c \approx 5$ K.

Finally, we note that the qualitative changes from 300 to 30 K in all spectra must clearly be connected to the low-frequency conductivity. At 300 K the carriers are localized on the dimers on the time scale of the spectroscopic measurement. Thus what is seen may basically be the intradimer transition with electron-phonon interference effects. The diminished thermal disorder at low temperature gradually allows the carriers to become delocalized, thus resulting in more Drude-like spectra. The detailed theoretical picture is unclear, but the data seem to indicate that electron-phonon as well as electron-electron interactions should be taken into account.

TABLE III. Totally symmetric (A_g) modes of BEDT-TTF, after Meneghetti *et al.* (Ref. 40).

Mode no.	Calculated frequency (cm^{-1})	Character
ν_1	2965	C—H stretch
ν_2	2926	C—H stretch
ν_3	1600	C=C stretch
ν_4	1549	C=C stretch
ν_5	1445	H—C—H bending
ν_6	1289	C—C—H bending
ν_7	1195	C—C—H bending
ν_8	1028	C—C stretch, C—C—H bending
ν_9	930	C—C stretch, C—C—H bending
ν_{10}	880	C—S stretch
ν_{11}	642	C—S stretch, C—C stretch
ν_{12}	478	C—S stretch
ν_{13}	457	C—S stretch
ν_{14}	373	Exterior ring deformation
ν_{15}	294	Exterior ring deformation
ν_{16}	156	Interior ring deformation
ν_{17}	28	Exterior ring deformation

V. CONCLUSIONS

In this paper we have presented and discussed the infrared spectra of two β -(ET) $_2$ X compounds. The data confirm the materials to be effectively two dimensional with a band-structure anisotropy of $\sim 2:1$. Average transfer integrals were derived for directions both along and perpendicular to the stacks. The anomalous room-temperature spectra may be related to localization of the carriers on the dimerized stacks. At low temperature the spectra are closer to what is expected for basically metallic behavior, although important electron-phonon and electron-electron interactions lead to deviations from the simple Drude model. Estimates of the intraband oscillator strength further suggest that short range electron-electron Coulomb correlations cannot be neglected.

ACKNOWLEDGMENTS

The authors thank Daniel Christensen and Flemming Nicolaisen, H. C. Ørsted Institute, for the loan of the Bruker Fourier transform spectrometer and for advice on its use. Niels Thorup is acknowledged for determining the crystal morphology. Work at Argonne has been supported by the U.S. Department of Energy, Office of Basic Energy Sciences, Division of Material Science, Contract No. W-31-109-ENG-38, while D.B.T. acknowledges support from the Danish Natural Science Research Council and from the National Science Foundation, Solid State Chemistry, Grant No. DMR-8416511. C.S.J. would like to thank the Royal Danish Academy of Sciences and Letters for support.

*Permanent address: Department of Physics, University of Florida, Gainesville, Florida 32611.

¹G. Saito, T. Enoki, K. Toriumi, and K. Inokuchi, *Solid State Commun.* **42**, 557 (1982).

²S. S. P. Parkin, E. M. Engler, R. R. Schumaker, R. Lagier, V. Y. Lee, J. C. Scott, and R. L. Greene, *Phys. Rev. Lett.* **50**, 270 (1983).

³E. B. Yagubskii, I. F. Shchegolev, V. N. Laukhin, P. A. Kononovich, M. V. Kartsovnik, A. V. Zvarykina, and L. I. Buravov, *Pis'ma Zh. Eksp. Teor. Fiz.* **39**, 12 (1984) [*JETP Lett.* **39**, 12 (1984)].

⁴K. Murata, M. Tokumoto, H. Anzai, H. Bando, G. Saito, K. Kajimura, and T. Ishiguro, *J. Phys. Soc. Jpn.* **54**, 1236 (1985). See also, J. E. Schirber, L. J. Azevedo, J. F. Kwak, E. L. Venturini, M. A. Beno, H. H. Wang, and J. M. Williams, *Solid State Commun.* **59**, 525 (1986).

⁵M. Tokumoto, K. Murata, H. Bando, H. Anzai, G. Saito, K. Kajimura, and T. Ishiguro, *Solid State Commun.* **54**, 1031 (1985).

⁶V. B. Ginodman, A. V. Gudenko, I. I. Zasavitskii, and E. B.

Yagubskii, *Pis'ma Zh. Eksp. Teor. Fiz.* **42**, 384 (1985) [*JETP Lett.* **42**, 472 (1985)].

⁷J. E. Schirber, L. J. Azevedo, J. F. Kwak, E. L. Venturini, P. C. W. Leung, M. A. Beno, H. H. Wang, and J. M. Williams, *Phys. Rev. B* **33**, 1987 (1986).

⁸E. B. Yagubskii, I. F. Shchegolev, S. I. Pesotskii, V. N. Laukhin, P. A. Kononovich, M. V. Kartsovnik, and A. V. Zvarykina, *Pis'ma Zh. Eksp. Teor. Fiz.* **39**, 275 (1984) [*JETP Lett.* **39**, 328 (1984)].

⁹J. M. Williams, H. W. Wang, M. A. Beno, T. J. Emge, L. M. Sowa, P. T. Copps, F. Behroozi, L. N. Hall, K. D. Carlson, and G. W. Crabtree, *Inorg. Chem.* **23**, 3839 (1984).

¹⁰H. H. Wang, M. A. Beno, U. Geiser, M. A. Firestone, K. S. Webb, L. Nuñez, G. W. Crabtree, K. D. Carlson, J. M. Williams, L. J. Azevedo, J. F. Kwak, and J. E. Schirber, *Inorg. Chem.* **24**, 2465 (1985).

¹¹V. F. Kaminskii, T. G. Prokhorova, R. P. Shibaeva, and E. B. Yagubskii, *Pis'ma Zh. Eksp. Teor. Fiz.* **39**, 15 (1984) [*JETP Lett.* **39**, 17 (1984)].

¹²J. M. Williams, T. J. Emge, H. H. Wang, M. A. Beno, P. T.

- Copps, L. N. Hall, K. D. Carlson, and G. W. Crabtree, *Inorg. Chem.* **23**, 2558 (1984).
- ¹³K. Mortensen, C. S. Jacobsen, K. Bechgaard, K. Carneiro, and J. M. Williams, *Mol. Cryst. Liq. Cryst.* **119**, 401 (1985).
- ¹⁴T. Mori, A. Kobayashi, Y. Sasai, H. Kobayashi, G. Saito, and H. Inokuchi, *Chem. Lett.* **1984**, 957 (1984).
- ¹⁵M.-H. Whango, J. M. Williams, P. C. W. Leung, M. A. Beno, T. J. Emge, H. H. Wang, K. D. Carlson, and G. W. Crabtree, *J. Am. Chem. Soc.* **107**, 5815 (1985).
- ¹⁶B. Koch, H. P. Geserich, W. Ruppel, D. Schweitzer, K. H. Dietz, and H. J. Keller, *Mol. Cryst. Liq. Cryst.* **119**, 343 (1985).
- ¹⁷H. Tajima, K. Yakushi, H. Kuroda, and G. Saito, *Solid State Commun.* **56**, 159 (1985).
- ¹⁸H. Kuroda, K. Yakushi, H. Tajima, and G. Saito, *Mol. Cryst. Liq. Cryst.* **125**, 135 (1985).
- ¹⁹M. G. Kaplunov, E. B. Yagubskii, L. P. Rosenberg, and Yu. G. Borodko, *Phys. Status Solidi A* **89**, 509 (1985).
- ²⁰T. Sugano, K. Yamada, G. Saito, and M. Kinoshita, *Solid State Commun.* **55**, 137 (1985).
- ²¹C. S. Jacobsen, J. M. Williams, and H. H. Wang, *Solid State Commun.* **54**, 937 (1985). Note that the polarizations || and \perp in that paper should be interchanged [Erratum: *Solid State Commun.* **57**, No. 8, p. i (1986)].
- ²²H. Tajima, H. Kanbara, K. Yakushi, H. Kuroda, and G. Saito, *Solid State Commun.* **57**, 911 (1986).
- ²³H. Tajima, H. Kanbara, K. Yakushi, H. Kuroda, and G. Saito, *Proceedings of the International Conference on Synthetic Metals, Kyoto, 1986* [*Synth. Met.* **19**, 137 (1987)].
- ²⁴C. S. Jacobsen, D. B. Tanner, J. M. Williams, and H. H. Wang, *Proceedings of the International Conference on Synthetic Metals, Kyoto, 1986* [*Synth. Met.* **19**, 125 (1987)].
- ²⁵T. J. Emge, H. H. Wang, M. A. Beno, P. C. W. Leung, M. A. Firestone, H. C. Jenkins, J. D. Cook, K. D. Carlson, J. M. Williams, E. L. Venturini, L. J. Azevedo, and J. E. Schirber, *Inorg. Chem.* **24**, 1736 (1985).
- ²⁶C. S. Jacobsen, D. B. Tanner, and K. Bechgaard, *Phys. Rev. B* **28**, 7019 (1983). [TMTSF is an abbreviation of tetramethyl-tetraselenafulvalene (C₁₀H₁₂Se₄) with the structural formula 2,2'-bi(4,5-dimethyl-1,3-diselenole-2-ylidene); TMTTF is tetramethyltetrathiafulvalene (C₁₀H₁₂S₄) of the same structure.]
- ²⁷See, for example, F. Wooten, *Optical Properties of Solids* (Academic, New York, 1972).
- ²⁸J. B. Torrance, B. A. Scott, and F. B. Kaufman, *Solid State Commun.* **17**, 1369 (1975).
- ²⁹P. F. Maldague, *Phys. Rev. B* **16**, 2437 (1977).
- ³⁰J. Tanaka, M. Tanaka, C. Tanaka, T. Ohno, T. Takabe, and H. Anzai, *Ann. N.Y. Acad. Sci.* **313**, 256 (1978). [TCNQ is an abbreviation for 7,7,8,8-tetracyanoquinodimethane (C₁₂H₄N₄) with the structural formula 2,2'-(2,5-cyclohexadiene-1,4-diylidene)bis(propanedinitrile-2-ylidene).]
- ³¹P. A. Lee, T. M. Rice, and P. W. Anderson, *Solid State Commun.* **14**, 703 (1974).
- ³²J. Hubbard, *Phys. Rev. B* **17**, 494 (1978).
- ³³H. Hinkelmann and H. G. Reik, *Solid State Commun.* **16**, 567 (1975).
- ³⁴D. B. Tanner, C. S. Jacobsen, J. M. Williams, and H. H. Wang (unpublished).
- ³⁵C. S. Jacobsen, *J. Phys. C* **19**, 5643 (1986).
- ³⁶V. A. Merzhanov, E. E. Kostyuchenko, O. E. Faber, I. F. Shchegolev, and E. B. Yagubskii, *Zh. Eksp. Teor. Fiz.* **89**, 292 (1985) [*Sov. Phys.—JETP* **62**, 165 (1985)].
- ³⁷G. R. Stewart, J. O'Rourke, G. W. Crabtree, K. D. Carlson, H. H. Wang, J. M. Williams, F. Gross, and K. Andres, *Phys. Rev. B* **33**, 2046 (1986).
- ³⁸S. Mazumdar and Z. G. Soos, *Phys. Rev. B* **23**, 2810 (1981).
- ³⁹C. B. Duke, N. O. Lipari, and L. Pietronero, *Chem. Phys. Lett.* **30**, 415 (1975).
- ⁴⁰M. Meneghetti, R. Bozio, and C. Pecile, *J. Phys. (Paris)* **47**, 1377 (1986).
- ⁴¹See, for example, R. Bozio and C. Pecile in *The Physics and Chemistry of Low-Dimensional Solids*, edited by L. Alcàcer, (Reidel, Dordrecht, 1980), p. 169.
- ⁴²T. Timusk, in *Low-Dimensional Conductors and Superconductors*, edited by L. Caron and D. Jérôme (Plenum, New York, 1987), and references therein.